Eur. Radiol. (2002) 12:568–574
DOI 10.1007/s003300100999

NEURO

M. El-Koussy
J. Mathis
K. O. Lövblad
F. Stepper
C. Kiefer
G. Schroth

Focal status epilepticus: follow-up by perfusion- and diffusion MRI

Received: 24 November 2000
Revised: 4 May 2001
Accepted: 10 May 2001
Published online: 7 July 2001

This paper was presented as part at the 2000 Meeting of the ESNR in Oslo, Norway, and was awarded the Poster Prize.

M. El-Koussy (✉) · K. O. Lövblad · C. Kiefer · G. Schroth
Department of Neuroradiology, University of Bern, Inselspital, Freiburgstrasse 4, 3010 Bern, Switzerland
E-mail: marwan.elkoussy@insel.ch
Phone: +41-31-6322655
Fax: +41-31-6324872

J. Mathis · F. Stepper
Department of Neurology, University of Bern, Inselspital, Freiburgstrasse 4, 3010 Bern, Switzerland

Abstract Diffusion-weighted MRI demonstrated bright right temporoparietal cortex, right hippocampus, and left cerebellum in a 63-year-old female suffering a focal convulsive status epilepticus. Hyperperfusion was noted in the right temporoparietal region. Two days later, a tendency to normalization of most of the diffusion and perfusion changes was noted, apart from the right hippocampus which became brighter on diffusion- and T2-weighted images. On the tenth day the apparent diffusion coefficient was slightly elevated, getting brighter on T2-weighted images with suspected mild post-contrast enhancement. We postulate that the discharging right hippocampus suffered cytotoxic edema, which later progressed to cell damage.

Keywords Status epilepticus · Diffusion-weighted MRI · Perfusion-weighted MRI · Cell death

Introduction

Recent echo-planar MRI techniques allow rapid acquisition of diffusion-weighted imaging (DWI) and perfusion images (PI). These techniques have been largely implemented in the setting of acute ischemic stroke. Diffusion abnormality could be seen within minutes after the ischemic insult as bright signal on DWI, accompanied by reduced apparent diffusion coefficient (ADC)values reflecting cytotoxic edema [1, 2]. Perfusion parameter maps presented evidence of regional hypoperfusion. Vasogenic edema becomes evident on the conventional T2 sequence 6–8 h after onset of ischemia as an area of bright signal [3]. Evaluation of status epilepticus includes clinical assessment, EEG, laboratory investigations (blood and CSF analysis), and neuroimaging modalities. Magnetic resonance imaging is indicated when seizures begin in adulthood or when evidence of focal onset has been found clinically or in the EEG. Only a few publications have focused on the role of DWI and PI in status epilepticus. Hyperperfusion of cerebral regions accompanying focal status epilepticus has already been demonstrated with the use of single-photon emission tomography (SPECT) [4] and PI on MRI [5]. Wieshmann et al. [6] and Lansberg et al. [7] described four cases of partial status epilepticus with

DWI abnormalities as well as abnormal findings on conventional MRI, MR angiography, and after gadolinium injection. Recently, Flacke et al. [8] documented reversible DWI and PI abnormalities in one case of nonconvulsive status epilepticus. These MRI abnormalities resolved completely with clinical recovery after anti-convulsant therapy. We report a case of convulsive partial status epilepticus evaluated by a combination of MRI modalities using conventional T1 and T2 sequences, DWI, PI, MR angiography, and post-gadolinium images and followed-up by another two MRI scans 2 and 9 days later.

Case report

A 63-year-old female suffered an acute onset of confusion and left-sided hemiparesis during lunch was admitted to the emergency unit. She had a 2-day history of acute partial hearing loss and a "common cold." On general examination the blood pressure and heart rate were elevated (blood pressure: 194/94 mmHg; heart rate: 120 beats/min). On neurological examination the patient had left-sided hemiparesis, neglect and hemianopsia, eye deviation to the left side, discontinuous jerky head movements to the left, as well as intermittent left-sided face twitches. The laboratory investigations showed elevated blood glucose level (7.98 mmol/l, normal range 3.66–5.55 mmol/l), explained by a history of latent diabetes mellitus managed by oral hypoglycemics. The only abnormality seen in the CSF analysis was the elevated glucose level (5.42 mmol/l, normal range 2.70–4.40 mmol/l). The patient had no past history of drug abuse.

The patient was transported to the MRI unit where she suffered a short attack of clonic convulsions involving the left side of the body. She then underwent an MRI examination (1.5 T; Magnetom Vision, Siemens, Erlangen, Germany) of the brain (scout at 2.42 p.m.). T1-weighted (TR/TE: 528/12 ms), proton-density (TR/TE: 3176/16 ms) and T2-weighted (TR/TE: 3176/98 ms) turbo spin-echo sequences were performed; these were supplemented by single-shot spin-echo echo-planar diffusion-weighted (b = 1000 s/mm^2) isotropic images (TR/TE: 5100/137 ms). Twenty axial images were acquired (slice thickness 5 mm; interslice gap 1.5 mm; field of view 240 mm; matrix size 96 × 200) with a total acquisition time of 20 s. The ADC maps were calculated. This was followed by administration of 15 ml. of gadopentate dimeglumine at a double dose of 0.2 mmol/kg (Gadovist, Schering, Berlin, Germany). Dynamic post-contrast T2* perfusion gradient-echo EPI images were acquired (TR/TE: 2000/60.7 ms). Twelve axial sections (slice thickness 5 mm; interslice gap 1.5 mm; field of view 240 mm; matrix size 128 × 128) were imaged 40 times every 2 s, with a total imaging time of 80 s. Finally, post-gadolinium T1-weighted (TR/TE: 672/17 ms) and MR angiography time-of-flight images (TR/TE: 35/6 ms) were acquired. Perfusion parameter maps, including the relative cerebral blood volume (rCBV), relative cerebral blood flow (rCBF), and transit time maps, including the time-to-peak (TTP), mean transit time (MTT), and time of arrival (TA), were then calculated on a separate offline workstation.

The conventional T1- and T2-series revealed no significant abnormality. The DWIs showed gyriform bright signal in the right temporoparietal cortex, where the ADC values (ADC: 0.694×10^{-3} mm^2/s) were decreased by approximately 38% in comparison with the contralateral side (ADC: 1.112×10^{-3} mm^2/s). The underlying white matter showed no significant diffusion abnormality. Another localized alteration of the diffusion state was seen in the left cerebellum (ADC: 0.754×10^{-3} mm^2/s) with an ADC decrease of approximately 20% in comparison with the right side (ADC: 0.943×10^{-3} mm^2/s). Bright signal on DWIs was also noticed in the right hippocampal region, with an ADC decrease of approximately 7% in comparison with the left side. The perfusion images revealed differential perfusion of both hemispheres with hyperperfusion of the right side (mainly the temporoparietal region; Fig. 1A). This was expressed by the elevated CBV and CBF, visible as higher signal intensity of the right hemisphere in comparison with the contralateral side (Table 1). The transit time maps (TA, TTP, and MTT) revealed faster arrival of the contrast bolus on the right side (Fig. 2). The MR angiography images showed higher signal of the right middle cerebral artery with obvious prominence of its M2 and M3 branches (Fig. 1B). No pathological enhancement could be seen on the post-contrast T1 images.

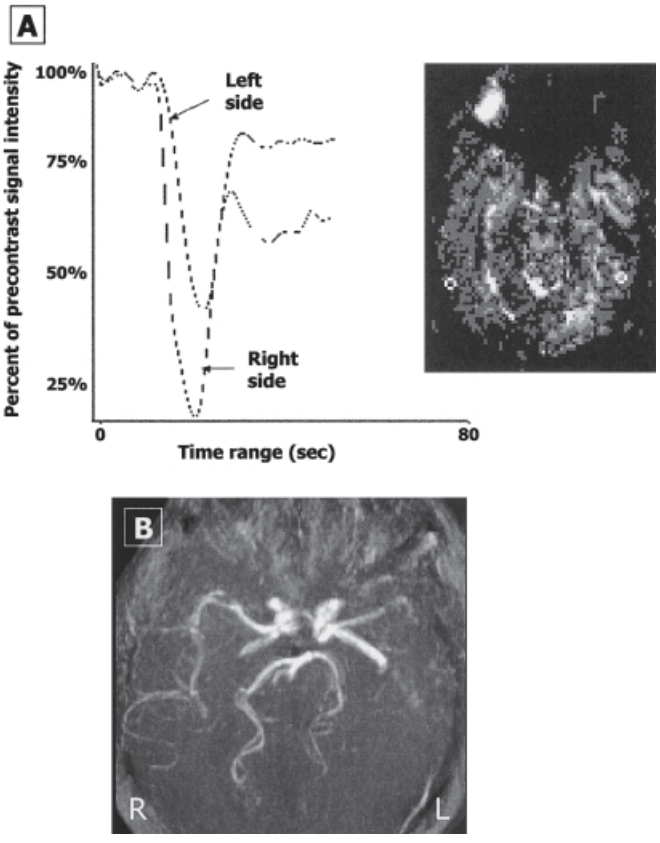

Fig. 1 The initial MRI study (day 1). **A** Signal-to-time curve obtained by placing two small regions of interest in the temporal cortex, each on one side. Lower signal is observed at each time point on the right side, reflecting higher relative cerebral blood volume. The time-to-peak (TTP) is also shifted to the left (reduced by ca. 2–3 s) in comparison with the left side. **B** An MR angiography shows the higher signal of the right middle cerebral artery with prominence of its branches

The EEG revealed focal "slow" activity on the right hemisphere, maximal in the anterior temporal region, spreading posteriorly (see Fig. 4, left). This was accompanied by periodically appearing blunted sharp wave complexes spreading to the parasagittal region, as well as partially to the contralateral temporal region. The left side showed a mixed alpha–beta, within the normal limits.

Table 1 The diffusion and perfusion parameters measured in the temporoparietal cortices, hippocampi, and cerebellar hemispheres of both sides on the first, third, and tenth days. The apparent diffusion coefficients were measured in $mm^2/s \times 10^{-6}$. The relative values of the cerebral blood flow and cerebral blood volume were calculated relative to the corresponding region on the unaffected left side. Time of arrival is measured in seconds

	Day 1	Day 3	Day 10
Apparent diffusion coefficient			
Right temporoparietal cortex	694	1016	1009
Left temporoparietal cortex	1112	987	1013
Right hippocampus	863	635	880
Left hippocampus	932	913	854
Right cerebellum	943	963	822
Left cerebellum	754	884	799
Relative cerebral blood flow			
Right temporoparietal cortex	1.504	1.422	1.092
Left temporoparietal cortex	1	1	1
Right hippocampus	1.216	1.402	1.032
Left hippocampus	1	1	1
Right cerebellum	1.206	1.067	1.011
Left cerebellum	1	1	1
Relative cerebral blood volume			
Right temporoparietal cortex	1.741	1.484	1.123
Left temporoparietal cortex	1	1	1
Right hippocampus	1.165	1.383	1.027
Left hippocampus	1	1	1
Right cerebellum	1.269	0.993	1.009
Left cerebellum	1	1	1
Time of arrival			
Right temporoparietal cortex	3.753	6.164	7.055
Left temporoparietal cortex	3.959	6.264	7.006
Right hippocampus	3.678	6.178	7.035
Left hippocampus	3.974	6.486	6.947
Right cerebellum	3.935	6.337	7.013
Left cerebellum	3.894	6.265	6.942

The clinical diagnosis was focal status epilepticus, but no definite precipitating factor could be found. Suspected causes included herpes simplex encephalitis and ischemic stroke; however, serum and CSF analysis, including the PCR results, performed on the second and seventh day after ictus, showed no evidence of herpes simplex infection. The seizures were controlled by anti-convulsant therapy. Sources of cardiac emboli were excluded by transesophageal echocardiography. Since the patient had no previous history of seizures, the acute onset of this first seizure activity with the hemisyndrome on the left side suggested the possibility of a cerebrovascular accident. Due to the unique diffusion and perfusion findings in the first MRI study and the asymmetry between the branches of the right middle cerebral artery and the left one on the MR angiography, conventional angiography was performed, in the search for vascular pathology. Gross vascular pathology of the carotid and vertebro-basilar systems was excluded by the cerebral angiography and Doppler sonography.

On the follow-up MRI 2 days after the initial MR examination, the diffusion abnormalities, seen previously in the cortex of the right temporoparietal region and left cerebellum, disappeared and the perfusion abnormalities were relatively less (Table 1). In contrast, the right hippocampal region became brighter on the DWIs, with a 30 % decrease of the ADC values (ADC: 0.635×10^{-3} mm^2/s) when compared with the contralateral side (ADC: 0.913×10^{-3} mm^2/s; Fig. 2) and demonstrated a mild increase in signal on T2-weighted images. On the plain T1-weighted images minimal swelling of the right hippocampal gyrus could be detected. Still, no definite pathological enhancement was detected on post-gadolinium T1 images. On this day, the patient was still drowsy. The EEG revealed continuous right-sided focal "slow" activity, present mainly in the right fronto-temporal region, with intermittent spread to the contralateral side, maximally to the frontal region. Frontal intermittent rhythmic delta activity (FIRDA-s) was noted bilaterally, reflecting widespread dysfunction of cortical and subcortical gray matter.

Another follow-up MRI scan was performed 1 week after the second scan and revealed apparent normalization of the signal of the right hippocampal lesion on diffusion-weighted images with the ADC values becoming minimally (ca. 3 %) higher than the left side. (Fig. 2) This lesion exhibited further increase in signal on the T2-weighted images with suspected faint punctate post-contrast enhancement (Fig. 3). Mild degree of lepto-meningeal enhancement was also noted (possibly due to the preceding lumbar puncture performed for CSF sampling). The EEG performed 1 day before the last MRI study revealed normal alpha–beta activity (max. frequency 20 Hz; Fig. 4, right). Intermittent rhythmic middle-high theta–delta waves (frequency 3–4 Hz) were present over the right temporal region.

Discussion

We describe one case of convulsive partial status epilepticus examined by multi-modality MRI, correlated with clinical and EEG findings. The MRI showed reversible perfusion changes in the discharging right temporoparietal region. Diffusion abnormalities in the right temporoparietal cortex and left cerebellum were also reversible, whereas the diffusion changes in the right hippocampus persisted till 9 days after ictus, and became evident on the conventional T2 series with punc-

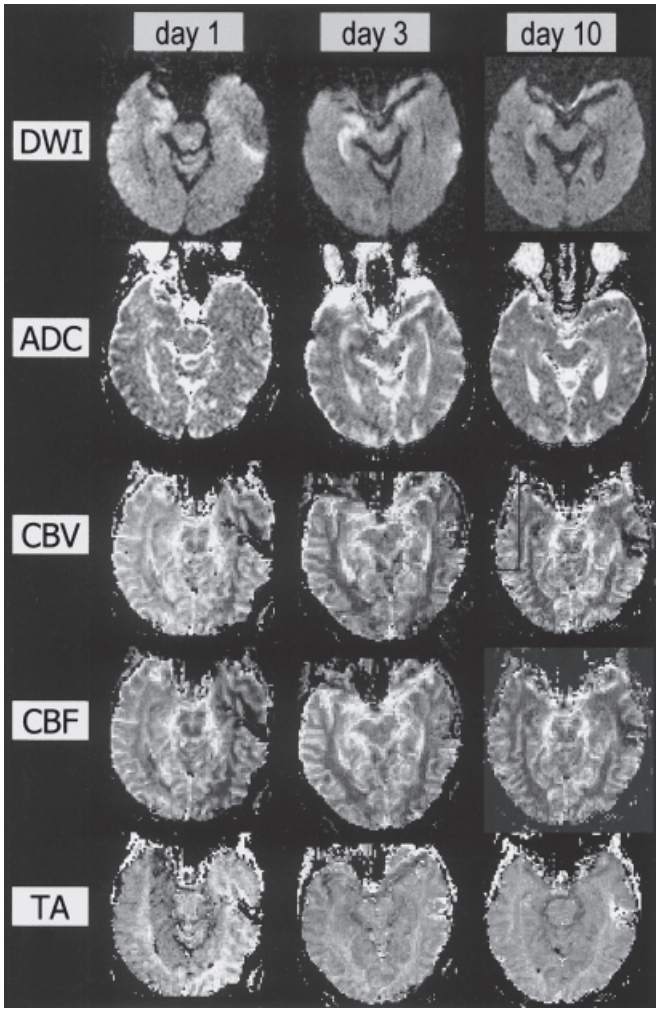

Fig. 2 Diffusion-weighted images (DWIs), apparent diffusion coefficient (ADC) maps, and perfusion parameter images acquired during the three MRI studies. Elevated cerebral blood volume *(CBV)* and cerebral blood flow *(CBF)*, accompanied by shortening of time of arrival *(TA)* in the right temporoparietal region was seen only on the first day. Note the bright signal on DWIs in the right temporoparietal cortex seen on day 1, which disappeared on the follow-up studies. The right hippocampus acquired its brightest signal on the second MRI examination. The accompanying localized depression of ADC values is noted as *dark signal* on the ADC maps

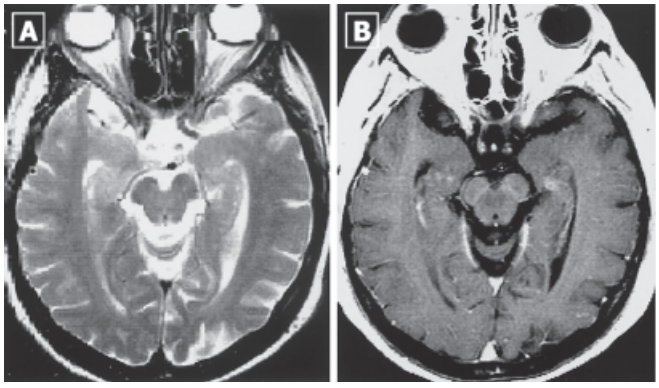

Fig. 3 The third MRI study (day 10). **A** Axial T2-weighted images showing a bright and swollen hippocampus on the right side. **B** The corresponding gadolinium-enhanced image demonstrates possible faint enhancement in the right hippocampus

tate post-contrast enhancement on post-gadolinium T1 series.

The hyperperfusion state of the discharging brain area, seen early in cases of status epilepticus, was previously documented by single photon emission computed tomography (SPECT) [4] and perfusion MRI [5]. Tc-99m-HMPAO brain SPECT proved to be unspecific in differentiating between ongoing focal status epilepticus and recently terminated status epilepticus; however, a SPECT scan demonstrating no area of focal hyperperfusion was considered to contradict the diagnosis of focal status epilepticus [4]. Warach et al. demonstrated the concordance of the perfusion MRI results with EEG, SPECT, and neurological signs. Their study showed elevated CBV and CBF on the affected side with symmetrical MTT on both sides [5]. In our case, the CBV and CBF were elevated concurrent with a decrease in the MTT, TTP, and TA in the affected brain region. The EEG findings corresponded well to these findings. Lee and Goldberg demonstrated a focal hyperperfusion pattern on carotid angiography in patients with status epilepticus [9]. The MR angiographic changes in the form of higher signal of the ipsilateral main artery with relative prominence of its branches in comparison with the other side, present in our report, were also noticed by Lansberg et al. [7]; however, such observations were absent in the case reported by Flacke et al. [8]. The elevated regional CBF, noted in sustained seizures, is explained by the elevation of local cerebral metabolic rate for oxygen and glucose and the resultant increase in blood supply [9, 10]. The perfusion changes in status epilepticus are different from the findings observed in ischemia, where the CBV and CBF are reduced with prolongation of the transit times [3].

The diffusion changes seen in status epilepticus have already been presented in the literature. In rats, ADC decreases of 14–49 % were observed during kainite- or flurothyl-induced status epilepticus [12, 13, 14]. In humans, gyriform bright signal was noted in the discharging cortex on DWI, without respect to vascular territories. The ADC values in the cortex showed a decrease, ranging from 18 to 36 %, in comparison with the normal side [6, 7, 8]. In addition to these findings, Wieshmann et al. reported a 31 % elevation of ADC in the white matter underlying the affected cortex, probably due to extracellular space expansion [6]. Lansberg et al. ob-

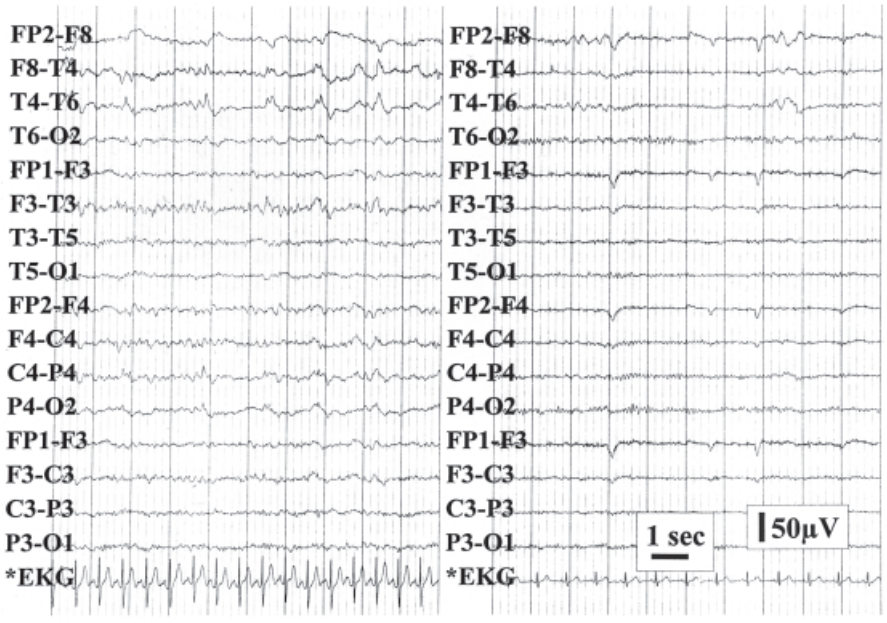

Fig. 4 The initial EEG recorded at the day of admission *(left side)* continuously showed a roughly periodic activity of middle-sized theta and blunted sharp waves in the right temporal region, maximal on T4 and much less in the left temporal region. The background activity was considered mildly to moderately abnormal on the right side. In context with the preceding clinical picture of left-sided twitches of the face, the diagnosis of subsiding partial status epilepticus could be confirmed. Particularly herpes simplex encephalitis was suggested as its cause. The control EEG 10 days later *(right side)* revealed a periodic appearance of rhythmic theta groups on the right temporal region and normalization of the background activity

served, in addition, hyperintensities on DWIs in remote regions, the ipsilateral thalamus, and contralateral cerebellum [7]. All forementioned abnormalities were reversible on follow-up scans after cessation of seizures. Only in one case in Lansberg et al.'s report was there elevation of the ADC and bright signal on T2* series on the late follow-up scan, reflecting neuronal cell death [7]. In our case, the diffusion changes in the right temporoparietal cortex (ADC decline of 38 %) were also reversible. Like in Lansberg et al.'s report [7], no diffusion abnormalities were identified in the subcortical white matter. Diffusion changes in remote regions were also observed (ADC depression in the left cerebellum) which also were reversible; however, the right hippocampus showed persistent diffusion changes, which lasted until the third MRI study (ninth day post ictus), accompanied by bright signal on T2-weighted images and punctate post-contrast enhancement. The ADCs showed tendency to normalization on the tenth day. These findings reflect an element of vasogenic edema, blood-brain barrier alterations, and neuronal damage. This ADC pattern of early postictal ADC depression, interictal normalization, and chronic elevation in the seizure focus has been reported previously [13]. Hugg et al. used DWI to lateralize intractable seizures in temporal lobe sclerosis. The ADCs were elevated in the ipsilateral hippocampus, where the side of the seizure focus was determined electrographically [15]. Wieshmann et al. also demonstrated elevation of the mean ADCs and decreased anisotropy index in hippocampi which fulfilled the MRI criteria of hippocampal sclerosis [16].

The mechanisms of the alteration of the diffusion status in status epilepticus include primary membrane permeability changes, with extracellular potassium accumulation and influx of Na^+ and Ca^{2+} ions accompanied by water shift to the intracellular space, leading to swelling of glial cells and neurons (cytotoxic edema) [10, 11]. Swelling of dendrites and astrocytes was demonstrated histologically in experimental studies [17]. A reduction of the extracellular compartment volume up to 30 % was reported [6, 7]. The reversibility of the diffusion abnormalities indicate that cytotoxic edema can be reversible, which was previously demonstrated histologically [18] and radiologically [12, 13, 14].

Prolonged seizures have long been known to be associated with cell injury and cell death in brain [19, 20, 21, 22, 23]. Histologically, some animal models showed neuronal cell death after status epilepticus [20, 24, 25]. Radiological evidence was reported by Meierkord et al. [19] who observed focal hyperintensities on T2-weighted images and local mass effect on angiography – consistent with edema – several days after onset of status epilepticus. On subsequent images, edema resolved, but atrophy and bright signal on T2-weighted images suggested gliosis [19]. The severity of neuronal cell damage is time dependent. The proposed cellular mechanisms include apoptosis and excitotoxic neuronal necrosis.[20, 21, 22, 26] Voltage-dependent Na^+ channels, glutamate receptors, nitric oxide (NO), and calcium ions may be involved in cellular damage [27, 28]. Because secretion levels of melatonin are decreased with aging, reductions in this pineal hormone may place neurons at a heightened risk for damage by excitatory synaptic transmission [27]. Moderate hypoxia was excluded as a risk factor for brain injury from status epilepticus [29]. In addi-

tion, elective vulnerability exists among the different populations of neurons. Animals exposed to kainic-acid induced status epilepticus display a striking pattern of selective neuronal vulnerability in the hippocampus. Neurons in the hilus/CA3 and CA1 subfields appear particularly sensitive, whereas dentate gyrus (DG) granule cells are resistant [23].

In our case report, we postulate that the seizure activity originated primarily in the right hippocampus with secondary activation of the ipsilateral cortex and contralateral cerebellum. These "secondary sites" initially suffered cytotoxic edema, which was reversed after antiepileptic therapy. In addition, the activated right hemisphere demonstrated a transient state of hyperperfusion. The right hippocampus initially suffered cytotoxic edema, which ultimately progressed to brain cell destruction. The cell damage in our case can be either explained by the effect of sustained seizures or by hypothesizing that this was originally an ischemic insult, which then triggered an attack of focal status epilepticus; however, the ischemic etiology can be excluded by the acute elevation of CBV and CBF, the MR angiography findings, the pattern of distribution of the decreased ADC values, not corresponding to a known vascular territory, as well as the negative findings on conventional angiography performed on the seventh day after ictus.

Acknowledgements The software used for image transfer (Sekt-Export) and computation of the perfusion parameter images (BiKe) was developed by U. Klose and B. Kardatzki (University of Tübingen, Germany).

References

1. Lovblad KO, Laubach HJ, Baird AE, Curtin F, Schlaug G, Edelman RR, Warach S (1998) Clinical experience with diffusion-weighted MR in patients with acute stroke. AJNR 19: 1061–1066
2. Weber J, Mattle HP, Heid O, Remonda L, Schroth G (2000) Diffusion-weighted imaging in ischaemic stroke: a follow-up study. Neuroradiology 42: 184–191
3. Beauchamp NJ Jr, Barker PB, Wang PY, vanZijl PC (1999) Imaging of acute cerebral ischemia. Radiology 212: 307–324
4. Tatum WO, Alavi A, Stecker MM (1994) Technetium-99m-HMPAO SPECT in partial status epilepticus. J Nucl Med 35: 1087–1094
5. Warach S, Levin JM, Schomer DL, Holman BL, Edelman RR (1994) Hyperperfusion of ictal seizure focus demonstrated by MR perfusion imaging. Am J Neuroradiol 15: 965–968
6. Wieshmann UC, Symms MR, Shorvon SD (1997) Diffusion changes in status epilepticus. Lancet 350: 493–494
7. Lansberg MG, O'Brian MW, Norbash AM, Moseley ME, Morell M, Albers GW (1999) MRI abnormalities associated with partial status epilepticus. Neurology 52: 1021–1027
8. Flacke S, Wüllner U, Keller E, Hamzei F, Urbach H (2000) Reversible changes in echo planar perfusion- and diffusion-weighted MRI in status epilepticus. Neuroradiology 42: 92–95
9. Lee SH, Goldberg HI (1977) Hypervascular pattern associated with idiopathic focal status epilepticus. Radiology 125: 159–163
10. McNamara JO (1994) Cellular and molecular basis of epilepsy. J Neurosci 14: 3413–3425
11. Lux HD, Heinemann U, Dietzel I (1986) Ionic changes and alterations in the size of extracellular space during epileptic activity. Adv Neurol 44: 619–639
12. Zhong J, Petroff OA, Prichard JW, Gore JC (1995) Barbiturate-reversible reduction of water diffusion coefficient in flurothyl-induced status epilepticus in rats. Magn Reson Med 33: 253–256
13. Righini A, Pierpaoli C, Alger JR, Chiro G di (1994) Brain parenchyma apparent diffusion coefficient alterations associated with experimental complex partial status epilepticus. Magn Reson Imaging 12: 865–871
14. Wang Y, Majors A, Najm I, Xue M, Comair Y, Modic M, Ng TC (1996) Postictal alterations of sodium content and apparent diffusion coefficient in epileptic rat brain induced by kainic acid. Epilepsia 37: 1000–1006
15. Hugg JW, Butterworth EJ, Kuzniecky RI (1999) Diffusion mapping applied to mesial temporal lobe epilepsy: preliminary observations. Neurology 53: 173–176
16. Wieshmann UC, Clark CA, Symms MR, Barker GJ, Birnie KD, Shorvon SD (1999) Water diffusion in the human hippocampus in epilepsy. Magn Reson Imaging 17: 29–36
17. Sperk G, Lassmann H, Baran H, Kish SJ, Seitelberger F, Hornykiewicz O (1983) Kainic acid induced seizures: neurochemical and histopathological changes. Neuroscience 10: 1301–1315
18. Griffiths T, Evans MC, Meldrum BS (1984) Status epilepticus: the reversibility of calcium loading and acute neuronal pathological changes in the rat hippocampus. Neuroscience 12: 557–567
19. Meierkord H, Wieshmann U, Niehaus L, Lehmann R (1997) Structural consequences of status epilepticus demonstrated with serial magnetic resonance imaging. Acta Neurol Scand 96: 127–132
20. Ingvar M, Morgan PF, Auer RN (1988) The nature and timing of excitotoxic neuronal necrosis in the cerebral cortex, hippocampus and thalamus due to flurothyl-induced status epilepticus. Acta Neuropathol 75: 362–369
21. Venero JL, Revuelta M, Machado A, Cano J (1999) Delayed apoptotic pyramidal cell death in CA4 and CA1 hippocampal subfields after a single intraseptal injection of kainate. Neuroscience 94: 1071–1081
22. Tuunanen J, Lukasiuk K, Halonen T, Pitkanen A (1999) Status epilepticus-induced neuronal damage in the rat amygdaloid complex: distribution, time-course and mechanisms. Neuroscience 94: 473–495
23. Becker AJ, Gillardon F, Blumcke I, Langendorfer D, Beck H, Wiestler OD (1999) Differential regulation of apoptosis-related genes in resistant and vulnerable subfields of the rat epileptic hippocampus. Brain Res Mol Brain Res 67: 172–176
24. Nevander G, Ingvar M, Auer R, Siesjo BK (1985) Status epilepticus in well-oxygenated rats causes neuronal necrosis. Ann Neurol 18: 281–290

25. Fujikawa DG (1996) The temporal evolution of neuronal damage from pilocarpine-induced status epilepticus. Brain Res 725: 11–22
26. Fujikawa DG, Shinmei SS, Cai B (1999) Lithium-pilocarpine-induced status epilepticus produces necrotic neurons with internucleosomal DNA fragmentation in adult rats. Eur J Neurosci 11: 1605–1614
27. Skaper SD, Ancona B, Facci L, Franceschini D, Giusti P (1998) Melatonin prevents the delayed death of hippocampal neurons induced by enhanced excitatory neurotransmission and the nitridergic pathway. FA status epilepticus. B J 12: 725–731
28. Kristian T, Siesjo BK (1998) Calcium in ischemic cell death. Stroke 29: 705–718
29. Sasahira M, Simon RP, Greenberg DA (1997) Neuronal injury in experimental status epilepticus in the rat: role of hypoxia. Neurosci Lett 222: 207–209